Cent. Eur. J. Eng. • 2(3) • 2012 • 383-391
DOI: 10.2478/s13531-012-0009-1

VERSITA

Central European Journal of **Engineering**

A power efficient bandwidth regulation technique for a low-noise high-gain RF wideband amplifier

Research article

Apratim Roy*, S.M.S. Rashid

Department of Electrical and Electronic Engineering, Bangladesh Univ. of Engineering and Technology (BUET), Dhaka-1000, Bangladesh

Received 01 February 2012; accepted 12 March 2012

Abstract: In this paper, a single-stage deep sub-micron wideband amplifier (LNA) using a reactive resonance tank and passive port-matching techniques is demonstrated operating in the microwave frequency range (K band). A novel power-efficient bandwidth (BW) regulation technique is proposed by incorporating a small impedance in the resonance tank of the amplifier configuration. It manifests a forward gain in the range of 5.9–10.7 dB covering a message bandwidth of 10.6–6.3 GHz. With regulation, input-output reflection parameters (S_{11}, S_{22}) and noise figure can be manipulated by -12.7 dB, -22.7 dB and 0.36 dB, respectively. Symmetric regulation is achieved for bandwidth and small signal gain with respect to moderate tank impedance (36.5% and -26.8%, respectively) but the effect on noise contribution remains relatively low (increase of 7% from a base value of 2.39 dB). The regulated architecture, when analyzed with 90 nm silicon CMOS process, supports low power (9.1 mW) on-chip communication. The circuit is tested with a number of combinations for tank (drain) impedance to verify the efficiency of the proposed technique and achieves better figures of merit when compared with published literature.

Keywords: Bandwidth regulation • Wideband amplifier • High gain • 90 nm

1. Introduction

A chief limiting factor hindering the downsizing of complementary metal-oxide-semiconductor (CMOS) integrated circuits has proven to be the additional delay associated with parasitic contributions of metal interconnects [1]. As a result, metallic interconnection schemes are being gradually replaced by wireless inter-chip and intra-chip communication standards, overcoming the limitation of speed in the process [2–4]. A popular technique employed in on-chip integrated wireless systems is ultra-wideband transmission (UWB), with features of immunity to interference, gigabit transmission speed, minimal effective power density, small antenna dimensions and provision for spread spectrum multiple access [5, 6]. A crucial component in the configuration of an inter-chip UWB wireless transceiver, along with transmitter pulse generation circuitry, is a low noise front-end amplifier [7]. To introduce wideband characteristics to this component, designers are always looking for raising the operating bandwidth of a receiver front-end and reducing its overall power requirements [8]. In this regard, K_u and K band frequencies (12–27 GHz) are deemed suitable for a microwave low noise amplifier for reliable high-speed short-distance transmission.

*E-mail: apratimroy45@gmail.com

To satisfy the diverse design criteria of a wideband receiver architecture (which may include standards like orthogonal multiplexing, impulse radio and rake receiver), gain and bandwidth regulation for the amplifier (LNA) gains critical importance [9]. An LNA also needs to provide low additional noise (apart from ambient contributions), lower port reflection, limited power dissipation and moderate-to-high small signal forward gain [10]. To meet these objectives, the research community is focusing on alternative technologies to silicon processes like silicon germanium (SiGe) and silicon on insulator (SOI), pushing up the manufacturing cost and making it difficult for the production assemblies to be economically efficient. Multistage topologies and transmission lines (TL) are integrated to enhance system performance in these technologies, increasing power demand or chip size and creating drawbacks for on-chip wireless standards [11–13]. A power-efficient CMOS microwave amplifier can contribute in avoiding these problems.

In this paper, a K band single-stage low power amplifier is proposed in a 90 nm CMOS silicon process with a passive port-matching network and an impedance based bandwidth regulation technique. Running on a 90 nm engine, the design exhibits a forward gain parameter (S_{21}) in the range of 6–11 dB at a 21.2 GHz operating frequency, with a bandwidth domain regulated around 6.3–10.6 GHz. Core power requirements (lower than 10 mW), center point (~21 GHz) and reverse isolation figure (S_{12}, ~-27 dB) for the amplifier remain largely unaffected by the regulation process whereas there are improvements in input reflection parameter (S_{11}, 26%) and stability from oscillation. Noise figure increases by 0.2 dB from the base value for moderate regulation and linear range for the amplifier input power improves significantly. The circuit remains stable on oscillatory behavior in the entire domain of concerned frequencies. It is verified that control of tank impedance of a low noise wideband amplifier can be an effective way of achieving higher bandwidth without significant loss of noise limit and gain, a highly desirable feature for applications like CDMA and on-chip gigabit interconnect systems.

2. Proposed architecture

Figure 1(a) presents a basic active wideband amplifier configuration where the common source topology with a driving device (T_1) is converted into a cascode structure through an isolating transistor (T_2). T_2 is designated as an insulating device because its main function is to prevent leakage in the reverse direction, thus separating the antenna and load ports. The structure uses a couple of coupling reactances (C_{in} and C_{out}), the device substrates are grounded and a resonance tank is formed

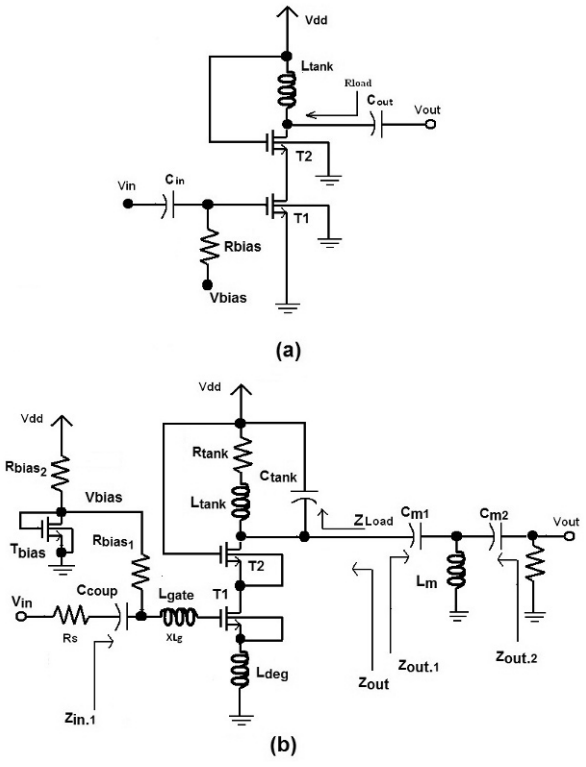

Figure 1. a) The basic common source unmatched (core) stacked amplifier; b) the proposed K-band single-stage matched wideband amplifier with a diode-connected biasing device

by the drain reactance L_{tank} and the gate-drain intrinsic parasitic capacitance of the isolating transistor. Fine tuning of the resonant frequency can be achieved by placing a parallel capacitor with the bank inductance (L_{tank}). The proposed K-band single stage low-power wideband amplifier is configured from this structure by appending port-matching networks, a parallel capacitor (C_{tank}) and a drain impedance (R_{tank}) in the resonance tank for the cascode amplifier. The matched and biased low-power amplifier with an adjustable 3-dB bandwidth is presented in Figure 1(b). For this amplifier construction, gate biasing for the cascode device (T_2) is supplied through the main power rail (V_{dd}). The diode-connected gate biasing transistor T_{bias} for the driving device (T_1) powers the concerned transistor through a moderate impedance R_{bias1} (~5KΩ) to ensure that gate bias supply does not interfere with small signal operation of the amplifier. The input matching network for the low noise amplifier consists of a degeneration inductor (L_{deg}), a gate reactance (L_{gate}) and an extra capacitor (C_{coup}) which provides a dual service of input coupling and matching the imaginary element of the RF-port impedance. Considering the intrinsic gate-source parasitic reactance ($C_{gs.T1}$) contributed by the driving tran-

sistor and the trans-conductance (mA/V) of the input device ($g_{m.T1}$), the input impedance of the wideband matched amplifier looking into the gate terminal of T_1 in Figure 1(b) will have the expression:

$$Z_{inp1} = f(L_{deg}, C_{gs.T1}) + jf(L_{deg}, L_{gate}, C_{gs.T1}, C_{coup}), \quad (1)$$

where

$$f(L_{deg}, C_{gs.T1}) = \frac{g_{mT1}L_{deg}}{C_{gs.T1}}, \quad and \quad (2)$$

$$f(L_{deg}, L_{gate}, C_{gs.T1}, C_{coup}) = \left[\omega\left(L_{deg} + L_{gate}\right)\right] - \frac{1}{\omega}\left(\frac{1}{C_{coup}} + \frac{1}{C_{gs.T1}}\right). \quad (3)$$

To eliminate the imaginary part of the input port-impedance L_{gate}, C_{coup} and the aspect ratio of T_1 are chosen to force

$$Z_{in.1} = Z_{inp.1}(\Re) = \frac{g_{mT1}L_{deg}}{C_{gs.T1}} = R_{source} = 50\Omega, \quad (4)$$

where R_{source} is the source resistance associated with input excitation in the front-end. In this arrangement, the cascode device (T_2) isolates the output from the input, allowing independent matching at the interfacing ports. The passive network for output port-matching is made with C_{m1}, C_{m2} and a nano-henry inductor (L_m) and resembles the shape of a "T" branch. After input matching is complete, output impedance of the RF port-matched amplifier (Z_{out}, see Figure 1(b)) approaches 100 Ω near the center frequency (21.2 GHz) whereas characteristic impedance for the following microwave load is supposed to be 50 Ω. If C_{m1} and C_{m2} are set in the fF (fermi-farad) range with L_m having a value of 1.1329 nH, then $Z_{out.1}$ is matched to core amplifier output impedance and the load sees the impedance $Z_{out.2}$ as a value close to 50 Ω. In this way, a resistance mirror at the output (laod) port extends the matching mechanism to K or K_u band frequencies [14]. Because of the absence of active buffer stages in the output linking circuit, the noise contribution of the amplifier observes significant savings.

The tank reactance (L_{tank}) resonating with gate-drain parasitic capacitance of T_2 and the tank capacitance (C_{tank}) settles the center frequency of the proposed amplifier in the K band (around 21 GHz). As quality factor for the tank impedance governs forward gain and feasible bandwidth from the amplifier, inclusion of a tank resistance (R_{tank}) can introduce regulation of the tank Q-factor, and hence regulation of the amplifier bandwidth. With a 90nm CMOS resistor model (*opppcres*), the tank impedance (R_{tank}) is controlled by its L/W ratio. During this process, $W_{R_{tank}}$ is manipulated between 5–40 µm while $L_{R_{tank}}$ is set to

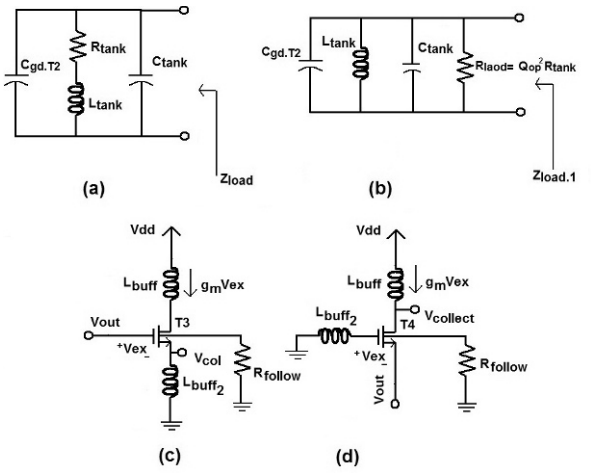

Figure 2. a) The load impedance network formed by the resonance tank; b) an equivalent model showing the effect of tank resistance on output load impedance; c) alternative source-follower output buffer; d) common-gate output buffer

1 µm. To derive a mathematical expression for the bandwidth regulation technique, the tank impedance formed by the resonance tank (Z_{load}) is shown in Figure 2(a), where $C_{gd.T2}$ [10] is the gate-drain capacitance generated in the isolating device and C_{tank} is a parallel tuning capacitor for the center frequency. Overall quality factor for the tuning inductor at the center frequency (ω_c) can be defined as

$$Q_{op} = \frac{\omega_c L_{tank}}{R_{tank}}, \quad (5)$$

and the equivalent load impedance (not including the parallel capacitor for simplification) in Figure 2(a) is expressed as

$$Z_{load}(s) = \frac{sL_{tank} + R_{tank}}{s^2 L_{tank} C_{gd2.T2} + sR_{tank} C_{gd2.T2} + 1}, \quad (6)$$

$$\approx \frac{sL_{tank}}{s^2 L_{tank} C_{gd2.T2} + sR_{tank} C_{gd2.T2} + 1}. \quad [for\ a\ small\ R_{tank}] \quad (7)$$

An alternate equivalent model for the tank is shown in Figure 2(b) with an independent tank resistance approximated by

$$R_{load} = Q_{op}^2 R_{tank}, \quad (8)$$

and the expression for the load impedance takes the form

$$Z_{load.1}(s) = \frac{sL_{tank}}{s^2 L_{tank} C_{gd2.T2} + \frac{sL_{tank}}{R_{load}} + 1}, \quad (9)$$

The condition to make the two networks shown in Figure 2(a) and 2(b) equivalent [15] is

$$Z_{load}(s) \approx Z_{load.1}(s), \tag{10}$$

and it can be satisfied by comparing equations (7) and (9) and making

$$sR_{tank}C_{gd2.T2} = s\frac{L_{tank}}{R_{load}} \tag{11}$$

$$or, R_{load} = \frac{L_{tank}}{R_{tank}C_{gd2.T2}} \tag{12}$$

$$= \frac{1}{L_{tank}C_{gd2.T2}}.\frac{{L_{tank}}^2}{{R_{tank}}^2}.R_{tank} \tag{13}$$

$$= (\omega_c \frac{L_{tank}}{R_{tank}})^2.R_{tank} \tag{14}$$

$$= {Q_{op}}^2.R_{tank}, \tag{15}$$

where the amplifier center frequency is given by

$$\omega_c^2 = \frac{1}{L_{tank}C_{gd2.T2}}. \tag{16}$$

So, equation (15) verifies the modeling in Figure 2(b) and suggests that adding a small drain impedance in the resonance bank is equivalent to increase in the parallel load as seen by a matched microwave output. As the gain and the 3 dB bandwidth depend conditionally on the effective output load, the extra tank resistance incorporates a bandwidth regulation technique for the proposed design. Equation (5) has defined the unloaded Q factor (Q_{op}) for the resonance bank formed on top of the insulating transistor. If we consider the influence of the output matching network and any loading capacitance, the loaded Q factor (Q_{loaded}) will take the form of

$$Q_{loaded} = \frac{Q_{op}}{1+\kappa}, \tag{17}$$

where κ is a coupling coefficient expressed in terms of unloaded and external (Q_{ext}) quality factors:

$$\kappa = \frac{Q_{op}}{Q_{ext}}. \tag{18}$$

Here, Q_{ext} depends on loading capacitors, center frequency and conductance offered by circuits connected at the load port [16]. If the port matching circuit eliminates the imaginary element for the output impedance $Z_{out.2}$ (in Figure 1(b)), then the gain of the amplifier will depend exclusively on the real component as seen by $Z_{out.2}$, which in turn will be influenced by the tank impedance. Equation (12) indicates that adding a tank resistance will reduce effective load resistance and gain of the core amplifier while boosting the message bandwidth. On the other hand, maximum forward gain and limited data bandwidth will follow in the absence of any extra drain resistance while the gain-bandwidth product remains as a constant. So, symmetric regulation of the bandwidth can be achieved by a suitable value of R_{tank} for the proposed design with only a minor sacrifice in terms of noise figure (if there is not any significant change in the bias current).

In lower operating frequencies, a source follower or a common gate configuration (as shown in Figure 2(c) and 2(d)) can be employed as buffer circuits for the output port in place of the proposed passive linking network. But as the operation moves to the K_u or K band, parasitic capacitances contributed by the active buffer device reduce the input impedance and subsequently the overall gain of the preceding amplifier. A significant portion of the available signal is also prone to drop in the buffer impedance, degrading the amplifier performance significantly. The proposed passive port-matching networks aim to remove this limitation while following the area restrictions imposed by an on-chip transceiver scheme.

3. Results and discussion

The designed single-stage low-noise wideband amplifier interfaced with matching networks is initially analyzed without any extra drain impedance (unregulated amplifier) on a Spectre platform using IBM 90 nm CMOS process parameters. The amplifier provides a relatively flat gain performance for K band frequencies when on-chip inductors are included in the design. The noise limit for the proposed architecture remain below 3 dB as it consumes about 9 mW of power.

3.1. Forward gain, reverse insulation and return loss

The open-load voltage gain of the proposed amplifier peaks at 20.1 dB with a relatively flat bandwidth of 6.1 GHz (from 20.9 to 27 GHz in the upper portion of the K band). On the other hand, small signal forward gain as measured by the S_{21} parameter attains a peak of 11 dB with a comparable bandwidth (~6.3 GHz, from 18.2 to 24.5 GHz) around the center frequency (21.2 GHz), as manifested by Figure 3(a). Because of the inclusion of passive matching circuits, the reverse isolation figure (S_{12}) is forced to stay below -26.7 dB in the 17 to 26 GHz range and the highest degree of isolation over the bandwidth settles at -32 dB.

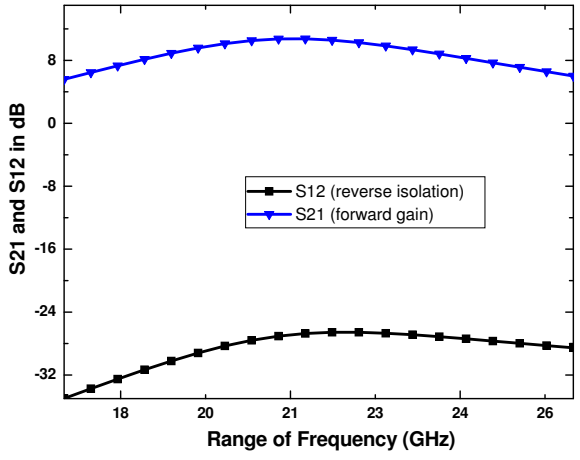

(a)

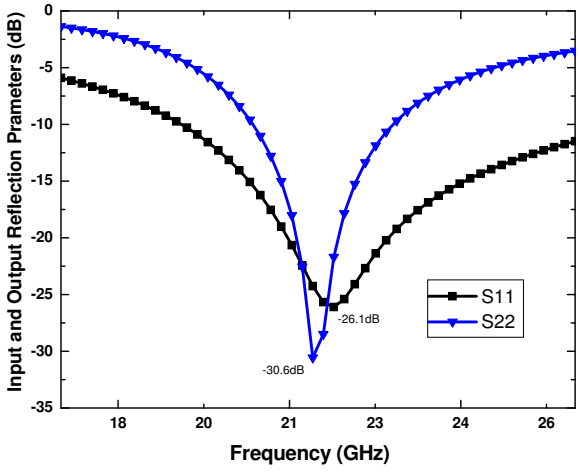

(b)

Figure 3. a) Forward gain (s_{21}) and reverse isolation (s_{12}) figures; b) port reflection parameters (for the unregulated amplifier).

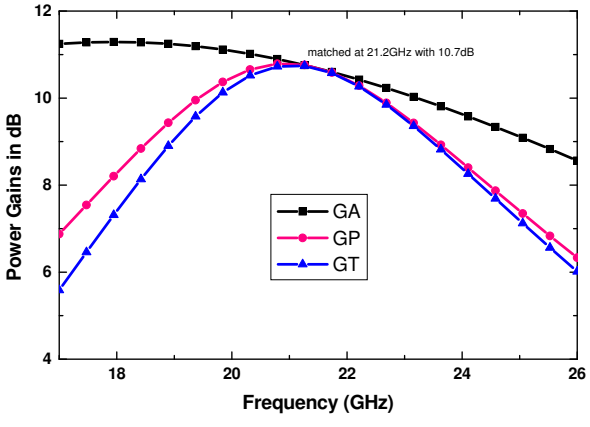

Figure 4. Power gains for the amplifier core and the matched LNA (without regulation).

These gain and isolation curves achieve perfect symmetry with respect to the maximum peak, indicating a balanced matching at port interfaces. The degenerated input matching network and the passive 'T' branch at the load port show their effects in Figure 3(b) as port return losses (S_{11} and S_{22}) remain below -8 and -3 dB in the 18–27 GHz band with dips occurring near 22 GHz around -26.1 dB and -30.6 dB, respectively.

3.2. Available, average and transducer gains

The three power gain parameters (available, average and transducer gains) for the amplifier are denoted by GA, GP and GT, respectively and tend to coincide near 10.7 dB around the center frequency, matching with the peak of the forward gain curve. Among these parameters, available power gain (GA) stays above 9.4 dB within the domain of achieved K-band bandwidth. In the same range, linking or matching networks modulate the base limit of average and transducer power gains to 8.5 and 7.8 dB, respectively (see Figure 4).

3.3. Bandwidth regulation for the RF amplifier

The unregulated amplifier response given in the two previous subsections in manipulated by inserting a small drain impedance (R_{tank} in Figure 1(b)) in the resonance tank of the core amplifier. A case of symmetric regulation is created by using a moderate value for R_{tank} ($L_{res} = 1$ µm and $W_{res} = 40$ µm for the resistive element), which raises the bandwidth by 37% while sacrificing the gain by 3 dB. The W_{res} parameter is further adjusted to explore the efficiency of the proposed technique and its effects on the microwave parameters are documented in Figures 5 to 8. In these figures, R_d denotes the appended extra tank impedance (R_{tank}).

3.3.1. Scattering parameters

The variation of the four scattering parameters under forced regulation is the subject of Figures 5 and 6. The extra drain impedance (with $W_{res} = 40$ µm, 20 µm) improves the peak isolation figure (S_{12}) from -27 dB to -31 dB. The dip in the input matching parameter (S_{11}) rises sharply from -26 to -39 dB but with a minimal right shift in the center frequency (about 400 MHz). The extent of output matching is degraded as S_{22} drops from -31 dB to -8 dB at 21.5 GHz. The 3 dB bandwidth increases by 4.3 GHz (68%) from 6.3 GHz (18.2 to 24.5 GHz) to 10.6 GHz as the peak gain (S_{21}) drops by 45% to 5.9 dB a the operating point, as shown in Figure 5(a).

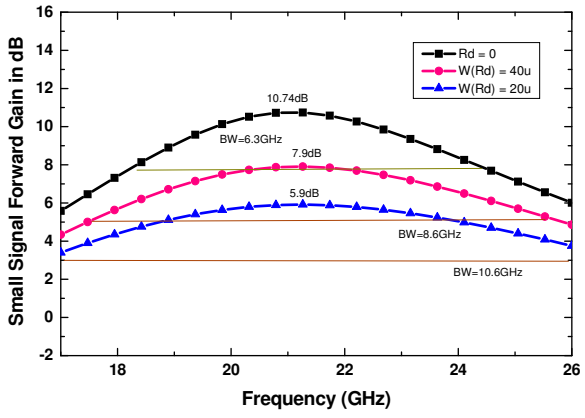

(a)

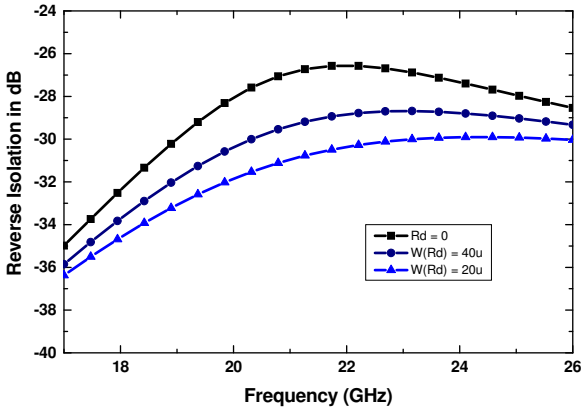

(b)

Figure 5. Effect of regulation on gain and bandwidth (as shown by a) S_{21} and b) S_{12}).

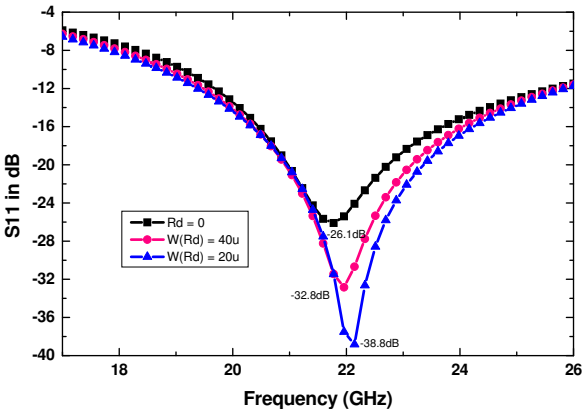

(a)

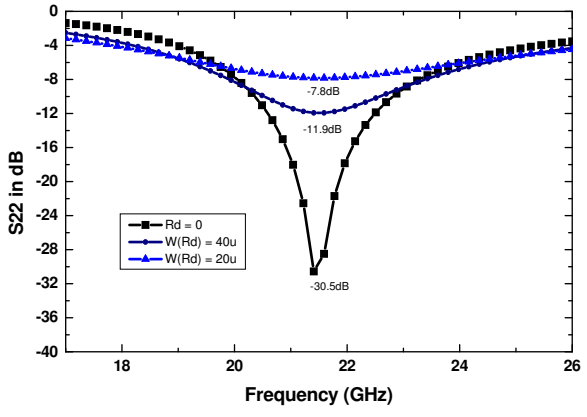

(b)

Figure 6. Effect of regulation (by R_{bank}) on the scattering reflection parameters, a)S_{11} and b) S_{22}.

3.3.2. Improvement of linearity

Without the drain impedance ($R_{bank} = 0$) the input referred 1 dB compression point (1 dB-CP) for the wideband amplifier stands near -15 dBm and increasing the bandwidth is expected to improve the linearity significantly as the range of input power for linear behavior is pushed up. This will be a peripheral advantage of the proposed regulation technique.

3.3.3. Low additional noise

As effective thermal noise contributed by the amplifier depends on the total resistance faced by the bias current, we expect the noise figure to move up when an additional drain impedance is included raising the overall bias resistance. Figure 7 shows the noise figure of the unregulated amplifier is below 3dB in the entire bandwidth. Regulation degrades the noise figure minimally by raising it from 2.39 dB to 2.58 dB (a rise of 7%). So there is not any significant degradation of the amplifier's noise performance

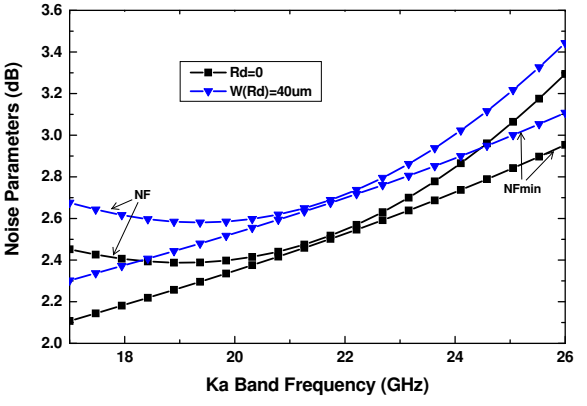

Figure 7. Noise contributions of the tank impedance (in terms of NF and NFmin).

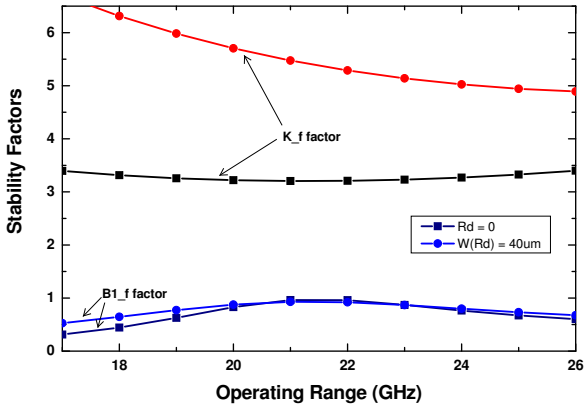

Figure 8. Upward shift in the Rollette stability factors (K_f and B_{1f})

with the introduction of the regulation technique and the pair of NF and NF_{min} still coincides near the center frequency. Among the active devices in the configuration, the driving transistor (T_1) contribute about 23% of the total white noise whereas the contribution of the isolating device (T_2) is 20%.

3.3.4. Effect on stability

The qualifying criterion for a microwave amplifier to be unconditionally stable requires the Roulette stability factor (K_f) to be greater than one and the B_{1f} factor to be greater than zero in all operating frequencies [10]. The simulated factor for the proposed design is greater than 3.2 from 17 to 26 GHz without the drain resistance. Regulation actually improves Rolette stability, making the base K_f value 4.89 over the concerned frequency domain (upper K-band). The effect of regulation on the B_{1f} factor is less prominent (peak remains near the value of 0.9) but still it clears the threshold limit comfortably. So, overall microwave stability for the wideband amplifier is improved by the proposed technique, as indicated by Figure 8.

3.3.5. Power penalty

Inclusion of a tank impedance in the demonstrated architecture is controlled in such a manner that it does not effect the overall bias current. As a result, the change in the consumption of power is only 80 µW even with forced regulation (W_{res} = 40 µm for R_{tank}). The 1.2 V dc bias supply spends below 10 mW for the matched amplifier with or without regulation. A stable bias current is maintained for the amplifier which only changes from 7.655 mA to 7.588 mA, resulting in power dissipations of 9.186 mW and 9.105 mW, respectively.

To summarize the results, the overall findings verify the proposed standard as a viable sub-micron mechanism to control the operating bandwidth of a low noise wideband amplifier.

4. Contrast with published results

Table 1 documents the synopsis of the 90 nm amplifier performance to make a comparative assessment with regard to published results of millimeter wave deep sub-micron amplifiers [11–13, 17–22] The proposed amplifier provides better port-isolation as calculated from the reflection parameters with low noise and reduced power penalty. To establish the relative merits of this microwave amplifier a figure of merit parameter (FOM) is defined by the equation

$$FOM = \frac{S_{21}(dB)Bandwidth(GHz)}{Power(mW)[NF(dB)-1]}, \qquad (19)$$

which is employed to assess the advantage of the regulated amplifier over its counterparts.

To prepare an appraisal of the degree of gain-bandwidth regulation achieved by the inserted drain impedance technique, variation of the microwave figures with percentage improvement is tabulated in table 2 for the amplifier. Inclusion of an extra tank resistance leads to an average change of 26% in the forward gain (approximated by S_{21} and the three power gains GA, GP, GT) while improving the 3dB bandwidth by 37%. Variations in the other figures also show improvements except in the case of reflection parameter at the output port (S_{22}), which drops sharply by 64%. The overall noise figure, a parameter which is most susceptible to any rise in equivalent bias impedance, increases in a much smaller scale (7.4%) and there is also improvement in range of linearity achieved by the amplifier. It is notable that power dissipated by the amplifier core remains at a relatively constant level despite the incorporation of forced regulation.

5. Conclusions

This paper proposes a novel bandwidth regulation technique for a 90nm CMOS wideband amplifier exploiting a cascode single-stage matched millimeter-wave (MMW) architecture. Use of passive resonance, degenerating and matching networks allow the amplifier to operate in the K band while its 3 dB effective bandwidth (EBW) is adjusted by 4.3 GHz around a center operating frequency of 21 GHz. Under the influence of an inserted drain resistor in the amplifier, symmetric regulation is achieved for forward gain and bandwidth with figures of -27% and 37%, respectively. When maximum regulation is enforced, input-output reflection parameters and base noise figure settle at

Table 1. Relative comparison of the proposed unregulated wideband amplifier with respect to published literature.

Reference	This Work	[11]	[12]	[13]	[17]	[18]	[19]	[20]	[21]	[22]
Technology(CMOS, nm)	90	130	130	90	130	90	180	130	180	180
Forward Gain (dB)	10.8	19	18.1	6.1	20	19	3.62	9	21	10
Center Frequency (GHz)	21.2	37	45	34	43	32.5	18.2	20	14.4	5.9
Bandwidth (GHz)	6.3	10	21	–	10	3	7.9	5.3	0.6	6.4
NF (dB)	2.39	–	8.2	–	6.3	3	0.42	5.5	8	5.35
Power (mW)	9.186	24	91.2	19	24	10	–	24	28	7
Reverse Isolation (S12, dB)	-26.7	–	–	–	–	–	-6.47	–	–	–
Input Isolation (S11, dB)	-26.1	<-15	<-20	-24	-16	<-8	-16.3	-9	-8	–
Output Isolation (S22, dB)	-33	< -15	-18	-19	-29	< -8	-7.71	-14	-15	–
No. of Stages	1	3	4	2	3	2	1	2	2	1
FOM (eq. 19)	5.33	–	0.58	–	1.57	2.85	–	0.44	0.06	2.1

Table 2. Effect of regulation on the proposed 90nm amplifier.

Microwave Figures	Without extra drain impedance (unregulated)	With Rd = R_{tank} (L_{res}=1μm, W_{res}=40μm)	Improvement (%)
Voltage Gain (VG, dB)	20.1	17.5	-12.9
Center Frequency for VG (GHz)	24.3	23.6	-2.9
Forward Gain (S_{21} in dB)	10.8	7.91	-26.8
Center Frequency for FG (GHz)	21.2	21.3	0.5
Bandwidth (GHz)	6.3	8.6	36.5
NF (dB)	2.39	2.58	-7.36
Power Dissipation (mW)	9.186	9.105	0.9
GA (dB)	10.8	8.22	-23.9
GP (dB)	10.8	7.93	-26.6
GT (dB)	10.8	7.91	-26.7
S_{11} (peak in dB)	-26.1	-32.9	26.1
S_{22} (peak in dB)	-33	-11.9	-63.9
$VSWR_1$ (dB)	0.845	0.805	–
$VSWR_2$ (dB)	1.197	2.412	–
K_f (Stability Factor, 17~26GHz)	>3.204	>4.89	52.6
B_{1f} (Stability Factor, 17~26GHz)	>0.31	>0.52	67.7
S_{12} (dB, in bandwidth)	< -26.7	<-28.7	–

-39 dB, -8 dB and 2.75 dB, respectively while linear range for the system remains unaffected. The gain-bandwidth regulation mechanism allows the proposed amplifier to be power-efficient (lower than 10 mW) and manipulates its message bandwidth without significant sacrifice of noise performance. Comparison with published data verifies the applicability of the mechanism for wireless interconnect standards.

Acknowledgments

The authors would like to thank Dr. H. Rashid and the authority of Bangladesh U. of Eng. and Tech. for extending their support and Intel BD. Association for financing the Cadence Tools.

References

[1] Saraswat K.C., Mohammadi F., Effect of interconnection scaling on time delay of VLSI circuits, IEEE TED, 1982, 29, 645–650

[2] Sun M., Zhang Y.P., Zheng G.X., Yin W.Y., Performance of Intra-Chip Wireless Interconnect Using On-Chip Antennas and UWB Radios, IEEE TAP, 2009, 57, 2756–2762

[3] Lager I.E., De Hoop A.T., Inter-chip and intra-chip pulsed signal transfer between transmitting and receiving loops in wireless interconnect configurations, In: Proceedings of European Microwave Conf. (Sept. 28–30, 2010 Paris France), 2010, 577–580

[4] Chang M.F., Roychowdhury V.P., Zhang L., Shin H., Qian Y., RF/wireless interconnect for inter- and intra-

chip communications, Proceedings of the IEEE, 2001, 89, 456–466

[5] Casu M.R., Durisi G., Implementation aspects of a transmitted-reference UWB receiver, Journal of Wireless Communications and Mobile Computing, 2005, 5, 551–566

[6] Malik W.Q., Stevens C.J., Edwards D.J., Multipath Effects in Ultrawideband Rake Reception, IEEE TAP, 2008, 56, 507–514

[7] Saha P.K., Sasaki N., Kikkawa T., A CMOS Monocycle Pulse Generation Circuit in a Ultra- Wideband Transmitter for Intra/Inter Chip Wireless Interconnection, Japanese Journal of Applied Physics, 2005, 44, 2104–2108

[8] Chen M., Lin J., A 0.1–20 GHz Low-Power Self-Biased Resistive-Feedback LNA in 90 nm Digital CMOS, IEEE MWCL, 2009, 19, 323–325

[9] Kim J., Hoyos S., Silva-Martinez J., Wideband Common-Gate CMOS LNA Employing Dual Negative Feedback With Simultaneous Noise, Gain, and Bandwidth Optimization, IEEE TMTT, 2010, 58, 2340–2351

[10] Leung B., VLSI for Wireless Communication, 1st ed., Prentice Hall India, New Delhi, 2002

[11] Doan C.H., Emami S., Niknejad A.M., Broadersen R.W., Millimeter-wave CMOS design, IEEE JSSC, 2005, 40, 144–155

[12] Wang T.P., Wang H., A Broadband 42–63 GHz Amplifier Using 0.13 μm CMOS Technology, In: Proceedings of IEEE/MTT-S Int. Microwave Symposium (June 3–8, 2007 Honolulu Hawaii), 2007, 1779–1782

[13] Masud M.A., Zirath H., Ferndahl M., Vickes H.O., 90 nm CMOS MMIC amplifier, In: Proceedings of IEEE RFIC Symp. (June 6–8, 2004 Fort Worth Texas), 2004, 201–204

[14] Rashid S., Ali S., Roy A., Rashid H., A 36.1 GHz Single Stage Low Noise Amplifier Using 0.13 μm CMOS Process, In: Proceedings of World Cong. on Comp. Science and Information Eng. (March 31–April 2, 2009 LA USA), 2009, 480–483

[15] Rashid S., Ali S., Roy A., Rashid H., Gain-Bandwidth Adjusting Techinque of A 36.1 GHz Single Stage Low Noise Amplifier Using 0.13 μm CMOS Process, In: Proceedings of Int. Conf. on Advanced Communication Tech. (Feb. 15–18, 2009 Phoenix Park Korea), 2009, 184–188

[16] Matthaei G.L., Young L., Jones E., Microwave Filters, Impedance-Matching Networks and Coupling Structures, New York: McGraw-Hill, 1964.

[17] Tsai J.H., Chen W.C., Wang T.P., *et al.*, A miniature Q-band low noise amplifier using 0.13 μm CMOS technology, IEEE MWCL, 2006, 16, 327–329

[18] Sanduleanu M.A.T., Zhang G., Long J.R., 31–34 GHz Low Noise Amplifier with On-chip microstrip Lines and Inter-stage Matching in 90nm Baseline CMOS, In: Proceedings of Radio Frequency Integrated Circuits Symp. (June 11–13, 2006 San Francisco California), 2006, 143–146

[19] Haque M.A., Hossain M.S., Ahmed S., Rashid H., 18.2 GHz Differential Low Noise Amplifier for On-Chip Ultra Wide Band Transceiver, In: Proceedings of IEEE Region 10 Conf. (Nov. 14–17, 2006 Hong Kong), 2006, 1–4

[20] Guo X., O K.K., A Power Efficient Differential 20 GHz Low Noise Amplifier With 5.3 GHz 3 dB Bandwidth, IEEE MWCL, 2005, 15, 603–605

[21] Floyd B., Shi L., Taur Y., Lagnado I., *et al.*, 15-GHz wireless interconnect implemented in a 0.18 μm CMOS technology using integrated transmitters, receivers, and antennas, In: Proceedings of VLSI Symp. Circuits (June 14–16, 2001 Kyoto Japan), 2001, 155–158

[22] Yu Y.H., Chen Y.J.E., Heo D., A 0.6 V low power UWB CMOS LNA, IEEE MWCL, 2007, 17, 229–231